



1                   **Future reduction of cold extremes over East Asia due to**  
2                   **thermodynamic and dynamic warming**

3 Donghuan Li<sup>1, 3</sup>, Tianjun Zhou<sup>2, 3, 5\*</sup>, Youcun Qi<sup>1, 3</sup>, Liwei Zou<sup>2</sup>, Chao Li<sup>4</sup>, Wenxia  
4 Zhang<sup>2</sup>, Xiaolong Chen<sup>2</sup>

5 <sup>1</sup>*Key Laboratory of Water Cycle and Related Land Surface Processes, Institute of Geographic*  
6 *Sciences and Natural Resources Research, Chinese Academy of Sciences, Beijing, China*

7 <sup>2</sup>*LASG, Institute of Atmospheric Physics, Chinese Academy of Science, Beijing, China*

8 <sup>3</sup>*University of Chinese Academy of Sciences, Beijing, China*

9 <sup>4</sup>*Max Planck Institute for Meteorology, Hamburg, Germany*

10 <sup>5</sup>*CAS Center for Excellence in Tibetan Plateau Earth Sciences, Chinese Academy of Sciences*  
11 *(CAS), Beijing, China*

12  
13 **Corresponding author:**

14 Dr. Tianjun ZHOU

15 LASG, Institute of Atmospheric Physics

16 Chinese Academy of Sciences

17 Beijing 100029, China.

18 Phone: 86-10-8299-5279

19 Fax: 86-10-8299-5172

20 E-mail: [zhoutj@lasg.iap.ac.cn](mailto:zhoutj@lasg.iap.ac.cn)

21

22



23

## Abstract

24 Cold extremes have large impacts on human society. Understanding the physical  
25 processes dominating the changes of cold extremes is crucial for a reliable projection  
26 of future climate change. The observed cold extremes have been decreased during last  
27 several decades and this trend will continue under the future global warming. Here, we  
28 quantitatively identify the contributions of dynamic (changes in large-scale atmospheric  
29 circulation) and thermodynamic (rising temperatures resulting from global warming)  
30 effects to East Asian cold extremes in the past several decades and in a future warm  
31 climate by using two sets of large ensemble simulation of climate models. We show  
32 that the dynamic component accounts for over 80% of the cold-month (coldest 5%  
33 boreal winter months) surface air temperature (SAT) anomaly in the past five decades.  
34 However, in a future warm climate, the thermodynamic change is the main contributor  
35 to the decreases in the intensity and occurrence probability of East Asian cold extremes,  
36 while the dynamic change is also contributive. The intensity of East Asian cold  
37 extremes will decrease by around 5°C at the end of the 21st century, in which the  
38 thermodynamic (dynamic) change contributes approximately 75% (25%). The present-  
39 day (1986-2005) East Asian cold extremes will almost never occur after around 2035,  
40 and this will happen eight years later due solely to thermodynamic change. The upward  
41 trend of a positive Arctic Oscillation-like sea level pressure pattern dominates the  
42 changes in the dynamic component. The finding provides a useful reference for  
43 policymakers in climate change adaptation activities.

44 **Key words:** East Asian cold extreme, dynamic adjustment, global warming



## 45 **1 Introduction**

46 Extreme events are widely concerned because of their high destructive power and  
47 great social impacts. Cold extremes have great impacts on agriculture, transportation, ,  
48 people's health and even cripple power supplies and led to rolling blackouts (Steponkus,  
49 1979; Andreescu and Frost, 1998; Sheridan et al., 2015; Thornton et al., 2016). The  
50 global mean surface air temperature (SAT) has been increasing in the past century due  
51 to the increase of anthropogenic greenhouse gas concentration in the atmosphere (Jones  
52 et al., 2008; IPCC, 2021). While warm extremes continue to attract considerable  
53 attention from the scientific community and ordinary people (e.g. Alexander et al., 2006;  
54 Rahimzadeh et al., 2009; Donat et al., 2012; Sun et al., 2014; Ma et al., 2017b), the cold  
55 extremes have also gained wide attention (e.g. Overland et al., 2011; Mori et al., 2014;  
56 Li et al., 2015; McCusker et al., 2016; Sun et al., 2016; Trenary et al., 2016; Ma et al.,  
57 2018; Qian et al., 2018) due to the mid-latitude cold extremes happened in recent  
58 several years.

59 A strong cold surge related to the negative phase of Arctic Oscillation (AO) and  
60 intensified Siberian High attacked North China during 6-8 January 2021. The  
61 temperatures reached or broke the records in more than 50 cities and counties. Beijing  
62 experienced the coldest day since 1951 on 7 January, with a daily minimum temperature  
63 of -19.6°C. (Wang et al., 2021; Zhou et al., 2022). The North America evidenced a  
64 widespread cold extreme in February 2021, which was caused by the distorted and  
65 weakened polar vortex (Lee, 2021; Lu et al., 2021). The temperatures were 15°C to  
66 25°C lower than normal in large areas and caused huge impacts on the energy supplies



67 and transportation (Zhou et al., 2022). Cold extreme occurs from time to time under  
68 global warming in recent years. Will it continue to occur if the global warming  
69 continues in the future?

70 The model simulations indicate that the anthropogenic influences have reduced  
71 the occurrence probability of cold extremes over eastern China with intensity stronger  
72 than the record-breaking cold extreme in January 2016 (Qian et al., 2018). The  
73 wintertime East Asian SAT is projected to increase significantly as a response to the  
74 future global warming (IPCC, 2021). Cold months defined based on the 20th century  
75 will be rarer under the future global warming (Räisänen and Ylhäisi, 2011) and the  
76 future warming will continuously reduce the intensity and occurrence probability of the  
77 cold extreme events (annual minimum daily minimum temperature) over East Asia  
78 (Kharin et al., 2013; 2018).

79 Previous studies demonstrated that the SAT is influenced by both the dynamic  
80 (changes in large-scale atmospheric circulation) and thermodynamic effects  
81 (Thompson et al., 2009; Cattiaux et al., 2010; Wallace et al., 2012; Smoliak et al., 2015;  
82 Deser et al., 2016). The dynamic effect, for example, the Arctic amplification, which  
83 reduces the polar-to-equator temperature gradient, can further modify the atmospheric  
84 circulation. There is a positive AO-like SLP (sea level pressure) changing pattern under  
85 the global warming (Fyfe et al., 1999; Yamaguchi and Noda, 2006; Kitoh, 2017) and  
86 the East Asian winter monsoon will be weakened in the warmer future conditions  
87 according to the multi-model simulations of the CMIP3 and CMIP5 models (Jiang and  
88 Tian, 2013; Xu et al., 2016). However, there is a lack of quantitative research on the



89 contributions of the dynamic and thermodynamic effects to the future changes of the  
90 East Asian cold extremes if the global mean SAT continues to increase.

91 The “dynamic adjustment” approaches (Wallace et al., 2012; Smoliak et al., 2015;  
92 Deser et al., 2016) have been proposed to divide the SAT anomaly into dynamic  
93 component (solely associated with circulation changes) and thermodynamic component  
94 (associated with thermodynamic processes). The dynamic adjustment of the North  
95 Hemisphere SAT field based on SLP can be used to investigate both the short-term  
96 climate fluctuations and long-term trends of SAT (Smoliak et al., 2015). Deser et al.  
97 (2016) indicates that the internal circulation trends accounts for over 30% of the North  
98 American wintertime warming trend in the past 50 years. The variability of circulation  
99 plays a critical role in the evolution of the East Asian winter temperature trends during  
100 1961-2018 and the internally induced dynamic component offsets the forced warming  
101 by over 70% in northern East Asia over the time period of 1979–2018 (Gong et al.,  
102 2019; 2021). The dynamic adjustment approach has also been used to investigate the  
103 wintertime precipitation changes and summertime SAT changes over East Asia (e.g.,  
104 Guo et al., 2019; Hu et al., 2019). However, these studies mainly focus on the mean  
105 temperature and mean precipitation changes in the past several decades, our knowledge  
106 on the contributions of the dynamic and thermodynamic effects to the future changes  
107 of the East Asian cold extremes associated with global warming remains quite limited.

108 By using two sets of grand ensemble simulations combined with observational  
109 data and reanalysis data, we aim to answer the following questions: (1) What are the  
110 relative contributions of the dynamic and thermodynamic effects to the East Asian cold



111 extremes in the past several decades? (2) How will the intensity and occurrence  
112 probability of East Asian cold extremes change in the warmer future? (3) What are the  
113 quantitative contributions of the dynamic and thermodynamic effects to the changes of  
114 East Asian cold extremes in the warmer future?

## 115 **2 Data and Methodology**

### 116 **2.1. Model Data**

117 The 100-member Grand Ensemble generated by the Max Planck Institute Earth  
118 System Model version 1.1 (MPI-GE; Maher et al., 2019) with horizontal resolution of  
119  $1.8^{\circ} \times 1.8^{\circ}$  and the 40-member Community Earth System Model Large Ensemble  
120 (CESM-LE; Kay et al., 2015) with horizontal resolution of  $1^{\circ} \times 1^{\circ}$  are applied in this  
121 study to investigate the contributions of dynamic and thermodynamic components to  
122 the East Asian cold extremes in recent decades and the future warm climate. The  
123 historical simulations integrated from 1850 to 2005 in the MPI-GE and from 1920 to  
124 2005 in the CESM-LE were driven by the observed forcings. The Representative  
125 Concentration Pathway 8.5 (RCP8.5) scenario simulations were performed from 2006  
126 to 2099 in the MPI-GE and from 2006 to 2100 in the CESM-LE. In addition, the 2000-  
127 yr MPI pre-industrial (PiCTL) simulation and 1800-yr CESM PiCTL simulation are  
128 also used in this study. For more detailed information of the MPI-GE and the CESM-  
129 LE, please refer to Maher et al. (2019) and Kay et al. (2015), respectively.

### 130 **2.2 Observation Data**

131 The following datasets are used in this study: (1) monthly mean SAT from the



132 Climatic Research Unit (CRU) version 4 with a horizontal resolution of  $0.5^{\circ} \times 0.5^{\circ}$   
133 (Harris et al., 2014). (2) Monthly mean three-dimensional circulation fields derived  
134 from the 20<sup>th</sup> Century Reanalysis (20CR) version 2 with a horizontal resolution of  $2^{\circ} \times 2^{\circ}$   
135 (Compo et al., 2011). The time period for these two datasets used in this study is from  
136 1920 to 2012.

### 137 **2.3 Dynamic Adjustment Approach**

138 The dynamic adjustment method presented by Deser et al. (2016) is based on the  
139 constructed circulation analogue using SLP. This method empirically divides SAT  
140 variability into dynamic component (associated with atmospheric circulation changes)  
141 and thermodynamic component (the residual part). The dynamic adjustment method is  
142 summarized below and please refer to Deser et al. (2016) for more details.

#### 143 **2.3.1 Application to the MPI-GE and CESM-LE**

144 For a given month and year (e.g. December 1990) in each ensemble member, we  
145 rank the 2000 (1800) December SLP fields in the PiCTL simulation by their similarity  
146 with the target SLP pattern according to Euclidean distance. Then, we randomly select  
147 100 SLP fields from the 150 closest SLP fields with smallest Euclidean distance to  
148 construct a best estimation of the target SLP pattern by linear combination. The same  
149 set of linear coefficients is applied to the accompanying SAT fields. We repeat the above  
150 procedure for 100 times and average the 100 linear combinations to derive the  
151 dynamically-induced SAT field in the target month. The multi-member mean of the  
152 dynamic component is regarded as the forced dynamic component and the internal



153 dynamic component is obtained by subtracting the forced part from the total dynamic  
154 component. Thermodynamic components are obtained as residuals (total minus  
155 dynamic) for both forced and internal components.

### 156 **2.3.2 Application to the observation**

157 There is no PiCTL simulation in the observation. Therefore, the quadratic trend of  
158 the SAT during 1920-2012 is first subtracted to obtain SAT series without  
159 anthropogenic forcing. For a given month and year, 40 SLP fields from 60 closest SLP  
160 fields are first selected (excluding the target month). Dynamic adjustment procedure is  
161 then applied to derive the dynamically-induced SAT fields in the observation.

162 To obtain the internal dynamic contribution to the observed SAT anomaly, a  
163 separate dynamic adjustment based on the internal component of the observed SLP  
164 anomalies is performed. The internal component of the observed SLP anomalies is  
165 obtained by subtracting the model ensemble-mean SLP anomaly from the observed SLP  
166 anomaly at each time step. Then, the forced dynamic component is calculated by  
167 subtracting the internal dynamic component from the total dynamic component.  
168 Thermodynamic components are obtained as residuals (total minus dynamic) for both  
169 forced and internal components.

### 170 **2.4 Baseline period and the study region**

171 The baseline period of 1986-2005 boreal winter is referred as the historical  
172 (present-day) climatology to investigate the SAT anomalies and contributions of  
173 dynamic and thermodynamic effects to future changes of East Asian cold extremes. The





174 certain region (the black box in Figure 2) from 20°N to 55°N and from 105°E to 130°E  
175 is regarded as East Asia in this study.

## 176 **2.5 The definitions of cold extreme and cold month**

177 The definition of East Asian cold extreme is as follows: in the models, the regional  
178 averaged monthly SAT anomaly of East Asia is firstly calculated. Then cold extremes  
179 are defined as the months in which the regional mean SAT is lower than the statistical  
180 5<sup>th</sup> percentile of the climatological monthly SAT series during DJF in a certain time  
181 slice. A month when cold extreme happens is defined as cold month. Similarly, the cold  
182 months in the observation are the 8 coldest months (5% of 150 winter months) during  
183 1962-2011 boreal winter (Table 1).

184 All the anomalies shown in this study are calculated relative to the climatological  
185 values of 1986-2005 boreal winter unless mentioned otherwise. Student's t test is  
186 applied to indicate the 5% significance level.

## 187 **2.6 The intensity and occurrence probability ratio of cold extreme**

188 The intensity of a cold extreme is the SAT deviation relative to the present-day  
189 boreal winter SAT climatology.

190 The occurrence probability ratio of the present-day cold extremes is calculated as  
191 follows (Ma et al., 2017a):

$$192 \quad PR = \frac{P_1}{P_0} \quad (1)$$

193 where PR is the occurrence probability ratio. The value of  $P_0$  is 5%, and  $P_1$  is the



194 probability of monthly SAT lower than the present-day cold extreme threshold in other  
195 time periods. For example, if the value of  $P1$  is 2% during a future period, then the  
196 value of PR is 0.4. For the calculation of occurrence probability ratio, we pull all the  
197 members together ratio rather than calculate it for each member.

### 198 **3 Results**

#### 199 **3.1 Dynamic and thermodynamic processes to East Asian cold extremes in recent** 200 **decades**

201 The winter temperature in East Asia shows obvious variability during 1962-2011  
202 boreal winter, and this is mainly caused by the dynamically-induced internal component.  
203 Moreover, this variability is the main cause of cold extremes over East Asia in the past  
204 five decades (Figure 1).

205 The decomposition of the observed East Asian cold-month SAT anomalies during  
206 1962-2011 boreal winter is shown in Figure 2a-c. The SAT is significantly lower than  
207 the present-day winter SAT climatology (more than 3°C) across the East Asian  
208 landmass (Figure 2a). The decomposition of SAT anomaly indicates that the cold  
209 extremes in recent decades are mainly caused by the dynamic component (Figure 2b  
210 and c), especially for the cold extremes happened in recent years. For example, the East  
211 Asian regional mean SAT anomaly in January 2011 is -3.47°C, in which, the dynamic  
212 component is -3.81°C, accounting up to 110% of the total SAT anomaly (Table 1).  
213 It is worth noting that these cold extremes are mainly caused by the internally-  
214 generated components, and the forced dynamic component shows little trend in the past



215 five decades and has little contribution to the observed cold extremes (Figure 1c and d).

216 The two sets of large ensemble model simulations can well reproduce the relative  
217 contributions of the dynamic and thermodynamic components to the cold extremes  
218 during 1962-2011 boreal winter (Figure 2d-i). The SAT is significantly lower than the  
219 winter SAT climatology throughout East Asia (Figure 2d and g) and the dynamic  
220 component is the main contributor to the cold extremes (Figure 2e, f, h and i). It should  
221 be noted that there are much more cold extreme samples in the MPI-GE and the CESM-  
222 LE, and the contribution of the dynamic component to the cold extremes are more  
223 evident in the two model ensembles than in the observation (Figure 2). The dynamic  
224 component accounts up to 85% and 82% of the total East Asian cold-month SAT  
225 anomaly during 1962-2011 boreal winter in the MPI-GE and the CESM-LE,  
226 respectively.

227 The results shown above indicate that the observed cold extremes in the past  
228 decades are mainly caused by the internal variability of atmospheric circulations. The  
229 cold extremes are often associated with strong East Asian winter monsoon flows, which  
230 are often accompanied with the blockings in the Urals and the intensified Siberian high.  
231 The composite circulation anomalies in the cold months during 1962-2011 boreal  
232 winter are further investigated (Figure 3). A ridge-trough pattern is seen over the  
233 Eurasian continent in the upper troposphere and there is southeastward propagation of  
234 wave activity flux (Figure 3a). The westerlies are weakened in the whole troposphere  
235 around 45°N -75°N, and there is an enhanced meandering flow pattern (Figure 3b). The  
236 weakened westerlies may favor the blocking events, which have strong relationship



237 with the cold extremes over East Asia. The surface Siberian High is intensified, and  
238 low-level northerly winds lead cold Arctic air spread southward to East Asia (Figure  
239 3c).

240 This typical type of circulation anomalies in cold months mentioned above are  
241 also well captured in the MPI-GE and the CESM-LE (Figure 3d-f). Namely, there is a  
242 ridge-trough pattern in the upper troposphere over the Eurasian continent and the  
243 surface Siberian High is enhanced. The westerlies are weakened in the whole  
244 troposphere and the cold air from the Arctic regions causes cold extremes over East  
245 Asia.

### 246 **3.2 Dynamic and thermodynamic contributions to the projected changes in East** 247 **Asian cold extremes**

248 In the observations, the dynamic component is the main contributor to the East  
249 Asian cold extremes in the past five decades. The human induced global warming has  
250 little effects on the changes in dynamically-induced SAT anomalies during 1962-2011  
251 (Figure 1). How will the dynamic and thermodynamic effects contribute to the future  
252 changes in cold extremes over East Asia?

253 We first examine the changes in the intensity of East Asian cold extremes (Figure  
254 4a and c). The SAT anomaly will continuously increase along with the global warming  
255 under the RCP8.5 scenario. Compared with the present day, the East Asian regional  
256 mean cold-month SAT will increase by approximately 4.8°C at the end of the 21<sup>st</sup>  
257 century according to the best estimation of MPI-GE (Figure 4a). The large center



258 locates in Northeast China, over 6°C (Figure 5a). The dynamic and thermodynamic  
259 components will also continually increase under the RCP8.5 scenario. The increases in  
260 the dynamic and thermodynamic components are approximately 1.3°C and 3.5°C at the  
261 end of the 21<sup>st</sup> century, respectively, in the MPI-GE (Figure 4a). Therefore, the  
262 contribution of the increase in dynamic component to the total SAT increase is 27%.  
263 The dynamic and thermodynamic components also increase faster in northern parts of  
264 East Asia than in other regions (Figure 5b and c). The faster increase of thermodynamic  
265 components in northern East Asia may be caused by the snow-albedo feedback, while  
266 the reason for the faster increase in dynamic component in this region is that the  
267 influence of East Asian Winter Monsoon on northern East Asia is more evident than on  
268 other subregions. The results in the CESM-LE are generally consistent with those in  
269 the MPI-GE. The East Asian regional mean SAT anomalies in cold months will increase  
270 by approximately 5.2°C at the end of the 21<sup>st</sup> century (Figure 4c). The corresponding  
271 increases in the dynamic and thermodynamic components are 1.3°C and 3.9°C,  
272 respectively. From the perspective of spatial distribution, the changing patterns of the  
273 total SAT and the dynamic component are similar in the two sets of large ensemble  
274 model simulations (Figure 5a, b, d and e). The thermodynamic component shows some  
275 differences (Figure 5c and f).

276 We extend the analysis from the changes in the intensity of cold extremes to the  
277 changes in the occurrence probability ratio of the present-day cold extremes in the  
278 future warm climate (Figure 4b). The 20-year running occurrence probability ratio of  
279 the present-day cold extremes will rapidly decrease under the RCP8.5 scenario in both



280 sets of the large ensemble model simulations. In the MPI-GE, the occurrence  
281 probability ratio of the present-day cold extremes will decrease to 0.05 in the period  
282 from 2034 to 2053 (Figure 4b), which means the present-day cold extremes will almost  
283 never occur after 2034. We isolate the dynamic and thermodynamic contributions to the  
284 changes of occurrence probability ratio of the present-day cold extremes. If we hold the  
285 dynamic component constant at the present-day level, and allow the thermodynamic  
286 component to evolve according to the model projection, the year when the occurrence  
287 probability ratio of the present-day cold extremes will decrease to 0.05 is 2042, eight  
288 years later than the time mentioned above (Figure 4b). Correspondingly, if we hold the  
289 thermodynamic component constant at the present-day level, and allow the dynamic  
290 component to evolve according to the model projection, the occurrence probability ratio  
291 of the present-day cold extremes will decrease to 0.2 at the end of the 21st century.  
292 From the perspective of spatial distribution, the occurrence probability ratio of the  
293 present-day cold extremes will be decreased to 0.05 before 2040 in parts of southeastern  
294 China, northeastern China and the Korean Peninsula (Figure 6a). The results in the  
295 CESM-LE are generally consistent with those in the MPI-GE (Figures 4d and 6b). The  
296 occurrence probability ratio of the present-day cold extremes will decrease to 0.05 in  
297 2035-2054 (Figure 4d) and the occurrence probability ratio also decreases faster in  
298 southeastern China, parts of northeastern China and the southern Korean Peninsula  
299 (Figure 6b). Different from the MPI-GE, occurrence probability ratio of the present-  
300 day cold extremes will decrease to 0.05 after 2060 in parts of North China and Northeast  
301 China in the CESM-LE (Figure 6b).



302           The thermodynamic change is the main contributor to the decreases in the intensity  
303 and occurrence probability of East Asian cold extremes, while the dynamic change is  
304 also contributive. We further examine the changes in SLP anomalies associated with  
305 East Asian cold extremes (Figures 7 and 8). Similar to the previous studies (Fyfe et al.,  
306 1999; Cai et al., 2017; Kitoh, 2017), the projected changes in SLP exhibit a positive  
307 AO-like pattern, particularly in the MPI-GE (Figure 7a and b). The winter-mean SLP  
308 will be reduced in the Arctic regions and enhanced in the mid-latitude regions. The AO  
309 shows highly positive correlation with the winter SAT anomaly over East Asia,  
310 especially the northern part, and the positive phase of AO is favorable for warm winter  
311 over East Asia (Gong et al., 2019; Wang et al., 2019). Similar SLP changing pattern  
312 also occurs in cold months (Figure 7c and d) and this is possibly the reason for the  
313 positive contribution of dynamic effects to the increase in SAT anomaly in cold months.  
314 We also construct the changes in the dynamic component of SLP (Figure 8). Changes  
315 in the dynamic component of SLP corroborates that the circulation changes are not  
316 favorable for the occurrence of East Asian cold extremes (Figure 8c and d).

## 317 **4 Summary and Discussion**

### 318 **4.1 Summary**

319           Based on the dynamic adjustment approach, we utilized two sets of large ensemble  
320 model simulations in the MPI-GE and CESM-LE to investigate the contributions of the  
321 background warming (thermodynamic effect) and circulation changes (dynamic effect)  
322 to the East Asian cold extremes. The contributions of the two components to the East



323 Asian cold extremes are quantitatively evaluated in the recent decades and under the  
324 future warming. The main conclusions are summarized as follows.

325 (1) The observed cold extremes in the past decades are mainly caused by the internal  
326 variability of atmospheric circulations, especially for the cold extremes happened  
327 in recent years. Both MPI-GE and the CESM-LE are consistent in revealing the  
328 typical circulation anomalies associated with the East Asian cold extremes. The  
329 relative contributions of the dynamic and thermodynamic components to the cold  
330 extremes are well captured in the two model ensembles, and the dynamic  
331 component accounts for more than 80% of the total cold-month SAT anomalies in  
332 the past five decades.

333 (2) In the future warm climate, the background warming is the main contributor to the  
334 decreases in the intensity and occurrence probability of East Asian cold extremes,  
335 while the circulation changes are also contributive. Compared with the present day,  
336 the mean intensity of the East Asian cold extremes will decrease by approximately  
337 5°C at the end of the 21<sup>st</sup> century under the RCP8.5 scenario and the dynamic  
338 component contributes to a quarter of this decrease. The occurrence probability  
339 ratio of the present-day cold extremes will almost never occur after around 2035,  
340 and if we hold the dynamic component constant at the present-day level, this will  
341 happen approximately 8 years later.

342 (3) Positive AO-like sea level pressure pattern upward trend is projected in both of the  
343 model ensembles, though there are a few differences between the two-ensemble





344 projection, and this change in large-scale circulation is unfavorable to the  
345 occurrence of East Asian cold extremes.

## 346 **4.2 Discussion**

347 Substantial efforts have been devoted so far to understand the response of climate  
348 extremes to global warming (e.g. Alexander et al., 2006; Sanderson et al., 2017; Zhang  
349 et al., 2018; AghaKouchak et al., 2020; Li et al., 2021), as well as their physical  
350 mechanisms (Cattiaux et al., 2010; Peing and Magnusdottir, 2014; Westra et al., 2014;  
351 Boschat et al., 2015; Horton et al., 2015; Qian et al., 2018). In particular, the  
352 thermodynamic processes (i.e., direct results of global warming) of changes in climate  
353 extremes have been well demonstrated. However, it remains ambiguous regarding how  
354 the dynamic processes will change under global warming, which is an important source  
355 of projection uncertainty for climate extremes (Shepherd, 2014; Norris et al., 2019).  
356 Hence, it is of vital importance to understand the dynamic changes of climate extremes,  
357 in order to improve the reliability of extreme climate projections.

358 In this study, we used two sets of large ensemble simulations data and dynamic  
359 adjust method to investigate the future change of cold extremes in East Asia, with a  
360 focus on understanding the thermodynamic and dynamic processes. Our results  
361 consistently show that the thermodynamic process is the dominant factor of future  
362 changes in East Asian cold extreme, with the contribution of dynamic process  
363 accounting for approximately one-quarter of the total change. In addition, the change  
364 in the dynamic component is attributed to the upward trend of a positive AO-like sea



365 level pressure pattern, and this has been supported by previous studies (Fyfe et al., 1999;  
366 Cai et al, 2017; Kitoh, 2017).

367 AO is the main circulation mode in the non-tropical regions of the Northern  
368 Hemisphere in winter (Thompson and Wallace, 1998), and has a significant impact on  
369 the winter climate in East Asia (Gong et al., 2001). However, it is worth noting that  
370 future winter temperature changes in East Asia may also be impacted by other large-  
371 scale circulation factors (Zhou et al., 2007; Cheung et al., 2012; He and Wang, 2013).  
372 The quantitative impacts of potential future changes of different circulation factors on  
373 cold extremes in East Asia remain unclear and require further investigation in future  
374 research.



375 **Data availability**

376 The MPI-GE experiment products can be downloaded from <https://esgf->  
377 [data.dkrz.de/search/mpi-ge/](https://data.dkrz.de/search/mpi-ge/). The specific experiments or variables can be selected  
378 through the navigation bar on the left-hand side. The monthly sea level pressure (psl),  
379 surface air temperature (tas), three-dimensional wind field (ua, va, wap), and  
380 geopotential height (zg) from the piControl, historical and rcp85 experiments are used  
381 in this work.

382 The CESM-LE experiment products can be downloaded from  
383 <https://www.earthsystemgrid.org/dataset/ucar.cgd.cesm4.cesmLE.html>.

384

385 **Author contribution**

386 TJZ designed the study. DHL performed the data analysis, produced the figures  
387 and wrote the manuscript draft. YCQ and CL collected the datasets. LWZ, WXZ and  
388 XLC contributed to the analysis methods. All the authors contributed to the discussion,  
389 writing, and editing of the manuscript.

390

391 **Competing interests**

392 The authors declare that they have no conflict of interest.

393

394 **Acknowledgments**

395 This work is jointly supported by the National Natural Science Foundation of  
396 China (Grant Nos. 42105031, 41988101).

397



398 **References**

- 399 AghaKouchak, A., Chiang, F., Huning, L. S., Love, C. A., Mallakpour, I., Mazdiyasni,  
400 O., ... & Sadegh, M. (2020). Climate extremes and compound hazards in a  
401 warming world. *Annual Review of Earth and Planetary Sciences*, 48, 519-548.  
402 <https://doi.org/10.1146/annurev-earth-071719-055228>.
- 403 Alexander, L. V., Zhang, X., Peterson, T. C., Caesar, J., Gleason, B., Klein Tank, A. M.  
404 G., ... & Vazquez - Aguirre, J. L. (2006). Global observed changes in daily climate  
405 extremes of temperature and precipitation. *Journal of Geophysical Research:*  
406 *Atmospheres*, 111(D5). <https://doi.org/10.1029/2005JD006290>
- 407 Andreescu, M. P., & Frost, D. B. (1998). Weather and traffic accidents in Montreal,  
408 Canada. *Climate research*, 9(3), 225-230. <https://doi.org/10.3354/cr009225>
- 409 Boschat, G., Pezza, A., Simmonds, I., Perkins, S., Cowan, T., & Purich, A. (2015).  
410 Large scale and sub-regional connections in the lead up to summer heat wave and  
411 extreme rainfall events in eastern Australia. *Climate Dynamics*, 44, 1823-1840.  
412 <https://doi.org/10.1007/s00382-014-2214-5>.
- 413 Cai, W., Li, K., Liao, H., Wang, H., & Wu, L. (2017). Weather conditions conducive to  
414 Beijing severe haze more frequent under climate change. *Nature Climate*  
415 *Change*, 7(4), 257-262. <https://doi.org/10.1038/nclimate3249>
- 416 Cattiaux, J., Vautard, R., Cassou, C., Yiou, P., Masson - Delmotte, V., & Codron, F.  
417 (2010). Winter 2010 in Europe: A cold extreme in a warming climate. *Geophysical*  
418 *Research Letters*, 37(20). <https://doi.org/10.1029/2010GL044613>



- 419 Cheung, H. N., Zhou, W., Mok, H. Y., & Wu, M. C. (2012). Relationship between Ural–  
420 Siberian blocking and the East Asian winter monsoon in relation to the Arctic  
421 Oscillation and the El Niño–Southern Oscillation. *Journal of Climate*, 25(12),  
422 4242–4257. <https://doi.org/10.1175/JCLI-D-11-00225.1>
- 423 Compo, G. P., Whitaker, J. S., Sardeshmukh, P. D., Matsui, N., Allan, R. J., Yin, X., ...  
424 & Worley, S. J. (2011). The twentieth century reanalysis project. *Quarterly Journal*  
425 of the Royal Meteorological Society, 137(654), 1–28.  
426 <https://doi.org/10.1002/qj.776>
- 427 Deser, C., Terray, L., & Phillips, A. S. (2016). Forced and internal components of winter  
428 air temperature trends over North America during the past 50 years: Mechanisms  
429 and implications. *Journal of Climate*, 29(6), 2237–2258.  
430 <https://doi.org/10.1175/JCLI-D-15-0304.1>
- 431 Donat, M. G., & Alexander, L. V. (2012). The shifting probability distribution of global  
432 daytime and night - time temperatures. *Geophysical Research Letters*, 39(14).  
433 <https://doi.org/10.1029/2012GL052459>
- 434 Fyfe, J. C., Boer, G. J., & Flato, G. M. (1999). The Arctic and Antarctic Oscillations  
435 and their projected changes under global warming. *Geophysical Research*  
436 *Letters*, 26(11), 1601–1604. <https://doi.org/10.1029/1999GL900317>
- 437 Gong, D. Y., Wang, S. W., & Zhu, J. H. (2001). East Asian winter monsoon and Arctic  
438 oscillation. *Geophysical Research Letters*, 28(10), 2073–2076.  
439 <https://doi.org/10.1029/2000GL012311>



- 440 Gong, H., Wang, L., Chen, W., & Wu, R. (2019). Attribution of the East Asian winter  
441 temperature trends during 1979–2018: Role of external forcing and internal  
442 variability. *Geophysical Research Letters*, 46(19), 10874-10881.  
443 <https://doi.org/10.1029/2019GL084154>
- 444 Gong, H., Wang, L., Chen, W., & Wu, R. (2021). Evolution of the East Asian winter  
445 land temperature trends during 1961–2018: role of internal variability and external  
446 forcing. *Environmental Research Letters*, 16(2), 024015. doi: 10.1088/1748-  
447 9326/abd586
- 448 Guo, R., Deser, C., Terray, L., & Lehner, F. (2019). Human influence on winter  
449 precipitation trends (1921–2015) over North America and Eurasia revealed by  
450 dynamical adjustment. *Geophysical Research Letters*, 46(6), 3426-3434.  
451 <https://doi.org/10.1029/2018GL081316>
- 452 Haarsma, R. J., Selten, F., Hurk, B. V., Hazeleger, W., & Wang, X. (2009). Drier  
453 Mediterranean soils due to greenhouse warming bring easterly winds over  
454 summertime central Europe. *Geophysical research letters*, 36(4).  
455 <https://doi.org/10.1029/2008GL036617>
- 456 Harris, I. P. D. J., Jones, P. D., Osborn, T. J., & Lister, D. H. (2014). Updated high -  
457 resolution grids of monthly climatic observations—the CRU TS3. 10  
458 Dataset. *International journal of climatology*, 34(3), 623-642.  
459 <https://doi.org/10.1002/joc.3711>
- 460 He, S., & Wang, H. (2013). Oscillating relationship between the East Asian winter



461 monsoon and ENSO. *Journal of Climate*, 26(24), 9819-9838.

462 <https://doi.org/10.1175/JCLI-D-13-00174.1>

463 Horton, D. E., Johnson, N. C., Singh, D., Swain, D. L., Rajaratnam, B., & Diffenbaugh,

464 N. S. (2015). Contribution of changes in atmospheric circulation patterns to

465 extreme temperature trends. *Nature*, 522(7557), 465-469.

466 <https://doi.org/10.1038/nature14550>

467 Hu, K., Huang, G., & Xie, S. P. (2019). Assessing the internal variability in multi-

468 decadal trends of summer surface air temperature over East Asia with a large

469 ensemble of GCM simulations. *Climate Dynamics*, 52(9), 6229-6242.

470 <https://doi.org/10.1007/s00382-018-4503-x>

471 IPCC. (2021). *Climate Change 2021. The Physical Science Basis. Contribution of*

472 *Working Group I to the Sixth Assessment Report of the Intergovernmental Panel*

473 *on Climate Change* [Masson-Delmotte, V., P. Zhai, A. Pirani, S.L. Connors, C.

474 Péan, S. Berger, N. Caud, Y. Chen, L. Goldfarb, M.I. Gomis, M. Huang, K. Leitzell,

475 E. Lonnoy, J.B.R. Matthews, T.K. Maycock, T. Waterfield, O. Yelekçi, R. Yu, and

476 B. Zhou (eds.)]. Cambridge University Press, Cambridge, United Kingdom and

477 New York, NY, USA, 2391 pp. doi:10.1017/9781009157896.

478 Jiang, D., & Tian, Z. (2013). East Asian monsoon change for the 21st century: Results

479 of CMIP3 and CMIP5 models. *Chinese Science Bulletin*, 58(12), 1427-1435.

480 <https://doi.org/10.1007/s11434-012-5533-0>

481 Jones, G. S., Stott, P. A., & Christidis, N. (2008). Human contribution to rapidly



- 482 increasing frequency of very warm Northern Hemisphere summers. *Journal of*  
483 *Geophysical Research: Atmospheres*, 113(D2).  
484 <https://doi.org/10.1029/2007JD008914>
- 485 Kay, J. E., Deser, C., Phillips, A., Mai, A., Hannay, C., Strand, G., ... & Vertenstein, M.  
486 (2015). The Community Earth System Model (CESM) large ensemble project: A  
487 community resource for studying climate change in the presence of internal  
488 climate variability. *Bulletin of the American Meteorological Society*, 96(8), 1333-  
489 1349. <https://doi.org/10.1175/BAMS-D-13-00255.1>
- 490 Kharin, V. V., Flato, G. M., Zhang, X., Gillett, N. P., Zwiers, F., & Anderson, K. J.  
491 (2018). Risks from climate extremes change differently from 1.5 C to 2.0 C  
492 depending on rarity. *Earth's Future*, 6(5), 704-715.  
493 <https://doi.org/10.1002/2018EF000813>
- 494 Kharin, V. V., Zwiers, F. W., Zhang, X., & Wehner, M. (2013). Changes in temperature  
495 and precipitation extremes in the CMIP5 ensemble. *Climatic change*, 119(2), 345-  
496 357. <https://doi.org/10.1007/s10584-013-0705-8>
- 497 Kitoh, A. (2017). The Asian Monsoon and its Future Change in Climate Models: A  
498 Review. *Journal of the Meteorological Society of Japan*, 95(1): 7-33.  
499 <https://doi.org/10.2151/jmsj.2017-002>
- 500 Lee, S. H. (2021). The January 2021 sudden stratospheric warming. *Weather*, 76(4),  
501 135-136. <https://doi.org/10.1002/wea.3966>
- 502 Li, C., Stevens, B., & Marotzke, J. (2015). Eurasian winter cooling in the warming





- 503 hiatus of 1998–2012. *Geophysical Research Letters*, 42(19), 8131-8139.  
504 <https://doi.org/10.1002/2015GL065327>
- 505 Li, C., Zwiers, F., Zhang, X., Li, G., Sun, Y., & Wehner, M. (2021). Changes in annual  
506 extremes of daily temperature and precipitation in CMIP6 models. *Journal of*  
507 *Climate*, 34(9), 3441-3460. <https://doi.org/10.1175/JCLI-D-19-1013.1>
- 508 Lu, Q., Rao, J., Liang, Z., Guo, D., Luo, J., Liu, S., ... & Wang, T. (2021). The sudden  
509 stratospheric warming in January 2021. *Environmental Research Letters*, 16(8),  
510 084029. doi: 10.1088/1748-9326/ac12f4
- 511 Ma, S., Zhou, T., Angélil, O., & Shiogama, H. (2017a). Increased chances of drought  
512 in southeastern periphery of the Tibetan Plateau induced by anthropogenic  
513 warming. *Journal of Climate*, 30(16), 6543-6560. [https://doi.org/10.1175/JCLI-D-](https://doi.org/10.1175/JCLI-D-16-0636.1)  
514 16-0636.1
- 515 Ma, S., Zhou, T., Stone, D. A., Angélil, O., & Shiogama, H. (2017b). Attribution of the  
516 July–August 2013 heat event in central and eastern China to anthropogenic  
517 greenhouse gas emissions. *Environmental Research Letters*, 12(5), 054020. doi:  
518 10.1088/1748-9326/aa69d2
- 519 Ma, S., Zhu, C., Liu, B., Zhou, T., Ding, Y., & Orsolini, Y. J. (2018). Polarized response  
520 of East Asian winter temperature extremes in the era of Arctic warming. *Journal*  
521 *of Climate*, 31(14), 5543-5557. <https://doi.org/10.1175/JCLI-D-17-0463.1>
- 522 Maher, N., Milinski, S., Suarez - Gutierrez, L., Botzet, M., Dobrynin, M., Kornblueh,  
523 L., ... & Marotzke, J. (2019). The Max Planck Institute Grand Ensemble: enabling



- 524 the exploration of climate system variability. *Journal of Advances in Modeling*  
525 *Earth Systems*, 11(7), 2050-2069. <https://doi.org/10.1029/2019MS001639>
- 526 McCusker, K. E., Fyfe, J. C., & Sigmond, M. (2016). Twenty-five winters of  
527 unexpected Eurasian cooling unlikely due to Arctic sea-ice loss. *Nature*  
528 *Geoscience*, 9(11), 838-842. <https://doi.org/10.1038/ngeo2820>
- 529 Mori, M., Watanabe, M., Shiogama, H., Inoue, J., & Kimoto, M. (2014). Robust Arctic  
530 sea-ice influence on the frequent Eurasian cold winters in past decades. *Nature*  
531 *Geoscience*, 7(12), 869-873. <https://doi.org/10.1038/ngeo2277>
- 532 Norris, J., Chen, G., & Neelin, J. D. (2019). Thermodynamic versus dynamic controls  
533 on extreme precipitation in a warming climate from the Community Earth System  
534 Model Large Ensemble. *Journal of Climate*, 32(4), 1025-1045.  
535 <https://doi.org/10.1175/jcli-d-18-0302.1>
- 536 Overland, J. E., Wood, K. R., & Wang, M. (2011). Warm Arctic—cold continents:  
537 climate impacts of the newly open Arctic Sea. *Polar Research*, 30(1), 15787.  
538 <https://doi.org/10.3402/polar.v30i0.15787>
- 539 Peings, Y., & Magnusdottir, G. (2014). Response of the wintertime Northern  
540 Hemisphere atmospheric circulation to current and projected Arctic sea ice decline:  
541 A numerical study with CAM5. *Journal of Climate*, 27(1), 244-264.  
542 <https://doi.org/10.1175/JCLI-D-13-00272.1>
- 543 Qian, C., Wang, J., Dong, S., Yin, H., Burke, C., Ciavarella, A., ... & Tett, S. F. (2018).  
544 Human Influence on the Record-breaking Cold Event in January of 2016 in



- 545 Eastern China. [in “Explaining Extreme Events of 2016 from a Climate  
546 Perspective”]. *Bulletin of the American Meteorological Society*, 99(1), S118-S122.  
547 <https://doi.org/10.1175/BAMS-D-17-0095.1>
- 548 Rahimzadeh, F., Asgari, A., & Fattahi, E. (2009). Variability of extreme temperature  
549 and precipitation in Iran during recent decades. *International Journal of*  
550 *Climatology: A Journal of the Royal Meteorological Society*, 29(3), 329-343.  
551 <https://doi.org/10.1002/joc.1739>
- 552 Räisänen, J., & Ylhäisi, J. S. (2011). Cold months in a warming climate. *Geophysical*  
553 *Research Letters*, 38(22). <https://doi.org/10.1029/2011GL049758>
- 554 Sanderson, B. M., Xu, Y., Tebaldi, C., Wehner, M., O'Neill, B., Jahn, A., ... & Lamarque,  
555 J. F. (2017). Community climate simulations to assess avoided impacts in 1.5 and  
556 2 C futures. *Earth System Dynamics*, 8(3), 827-847. [https://doi.org/10.5194/esd-](https://doi.org/10.5194/esd-8-827-2017)  
557 [8-827-2017](https://doi.org/10.5194/esd-8-827-2017)
- 558 Shepherd, T. G. (2014). Atmospheric circulation as a source of uncertainty in climate  
559 change projections. *Nature Geoscience*, 7(10), 703-708.  
560 <https://doi.org/10.1038/ngeo2253>
- 561 Sheridan, S. C., & Allen, M. J. (2015). Changes in the frequency and intensity of  
562 extreme temperature events and human health concerns. *Current Climate Change*  
563 *Reports*, 1(3), 155-162. <https://doi.org/10.1007/s40641-015-0017-3>
- 564 Smoliak, B. V., Wallace, J. M., Lin, P., & Fu, Q. (2015). Dynamical adjustment of the  
565 Northern Hemisphere surface air temperature field: Methodology and application



566 to observations. Journal of Climate, 28(4), 1613-1629.  
567 <https://doi.org/10.1175/JCLI-D-14-00111.1>

568 Steponkus, P. L. (1979). Cold hardiness and freezing injury of agronomic  
569 crops. *Advances in Agronomy*, 30, 51-98. [https://doi.org/10.1016/S0065-](https://doi.org/10.1016/S0065-2113(08)60703-8)  
570 [2113\(08\)60703-8](https://doi.org/10.1016/S0065-2113(08)60703-8)

571 Sun, L., Perlwitz, J., & Hoerling, M. (2016). What caused the recent “Warm Arctic,  
572 Cold Continents” trend pattern in winter temperatures?. *Geophysical Research*  
573 *Letters*, 43(10), 5345-5352. <https://doi.org/10.1002/2016GL069024>

574 Sun, Y., Zhang, X., Zwiers, F. W., Song, L., Wan, H., Hu, T., ... & Ren, G. (2014). Rapid  
575 increase in the risk of extreme summer heat in Eastern China. *Nature Climate*  
576 *Change*, 4(12), 1082-1085. <https://doi.org/10.1038/nclimate2410>

577 Thompson, D. W., & Wallace, J. M. (1998). The Arctic Oscillation signature in the  
578 wintertime geopotential height and temperature fields. *Geophysical research*  
579 *letters*, 25(9), 1297-1300. <https://doi.org/10.1029/98GL00950>

580 Thompson, D. W., Wallace, J. M., Jones, P. D., & Kennedy, J. J. (2009). Identifying  
581 signatures of natural climate variability in time series of global-mean surface  
582 temperature: Methodology and insights. *Journal of Climate*, 22(22), 6120-6141.  
583 <https://doi.org/10.1175/2009JCLI3089.1>

584 Thornton, H. E., Hoskins, B. J., & Scaife, A. A. (2016). The role of temperature in the  
585 variability and extremes of electricity and gas demand in Great  
586 Britain. *Environmental Research Letters*, 11(11), 114015. doi: 10.1088/1748-



- 587           9326/11/11/114015
- 588   Trenary, L., DelSole, T., Tippett, M. K., & Doty B. (2016). Extreme Eastern US Winter  
589           of 2015 Not Symptomatic of Climate Change [in “Explaining Extreme Events of  
590           2016 from a Climate Perspective”]. *Bulletin of the American Meteorological*  
591           *Society*, 97(12), S31-S35. doi: 10.1175/BAMS-D-16-0156.1
- 592   Wallace, J. M., Fu, Q., Smoliak, B. V., Lin, P., & Johanson, C. M. (2012). Simulated  
593           versus observed patterns of warming over the extratropical Northern Hemisphere  
594           continents during the cold season. *Proceedings of the National Academy of*  
595           *Sciences*, 109(36), 14337-14342. <https://doi.org/10.1073/pnas.1204875109>
- 596   Wang, C., Yao, Y., Wang, H., Sun, X., & Zheng, J. (2021). The 2020 summer floods and  
597           2020/21 winter extreme cold surges in China and the 2020 typhoon season in the  
598           western North Pacific. *Advances in Atmospheric Sciences*. 38, 896 – 904.  
599           <https://doi.org/10.1007/s00376-021-1094-y>
- 600   Wang, L., Deng, A., & Huang, R. (2019). Wintertime internal climate variability over  
601           Eurasia in the CESM large ensemble. *Climate dynamics*, 52(11), 6735-6748.  
602           <https://doi.org/10.1007/s00382-018-4542-3>
- 603   Westra, S., Fowler, H. J., Evans, J. P., Alexander, L. V., Berg, P., Johnson, F., ... &  
604           Roberts, N. (2014). Future changes to the intensity and frequency of short -  
605           duration extreme rainfall. *Reviews of Geophysics*, 52(3), 522-555.  
606           <https://doi.org/10.1002/2014RG000464>
- 607   Xu, M., Xu, H., & Ma, J. (2016). Responses of the East Asian winter monsoon to global



608 warming in CMIP5 models. *International Journal of Climatology*, 36(5), 2139-  
609 2155. <https://doi.org/10.1002/joc.4480>

610 Yamaguchi, K., & Noda, A. (2006). Global warming patterns over the North Pacific:  
611 ENSO versus AO. *Journal of the Meteorological Society of Japan. Ser. II*, 84(1),  
612 221-241. <https://doi.org/10.2151/jmsj.84.221>

613 Zhang, W., Zhou, T., Zou, L., Zhang, L., & Chen, X. (2018). Reduced exposure to  
614 extreme precipitation from 0.5C less warming in global land monsoon  
615 regions. *Nature Communications*, 9(1), 3153. [https://doi.org/10.1038/s41467-](https://doi.org/10.1038/s41467-018-05633-3)  
616 018-05633-3

617 Zhou, T., Zhang, W., Zhang, L., Clark, R., Qian, C., Zhang, Q., ... & Zhang, X. (2022).  
618 2021: A Year of Unprecedented Climate Extremes in Eastern Asia, North America,  
619 and Europe. *Advances in Atmospheric Sciences*. 39, 1598 - 1607.  
620 <https://doi.org/10.1007/s00376-022-2063-9>

621 Zhou, W., Li, C., & Wang, X. (2007). Possible connection between Pacific oceanic  
622 interdecadal pathway and East Asian winter monsoon. *Geophysical Research*  
623 *Letters*, 34(1). <https://doi.org/10.1029/2006GL027809>

624

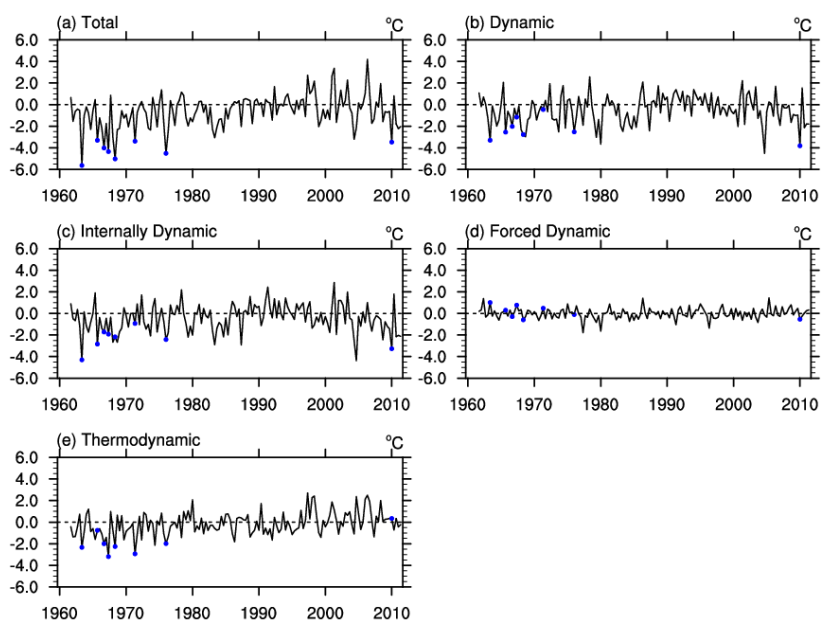
625



626 **Table 1** The list of observed cold months in period of 1962-2011 boreal winter.

Time (Year Month)	Total(°C)	Dynamic(°C)	Thermodynamic(°C)	Dynamic ratio(%)
196402	-5.63	-3.30	-2.33	58.6
196902	-5.02	-2.77	-2.25	55.1
197701	-4.51	-2.52	-1.98	56.0
196802	-4.35	-1.16	-3.19	26.6
196712	-4.01	-2.02	-2.00	50.3
201101	-3.47	-3.81	0.34	109.9
197202	-3.39	-0.45	-2.93	13.4
196612	-3.30	-2.55	-0.75	77.1

627

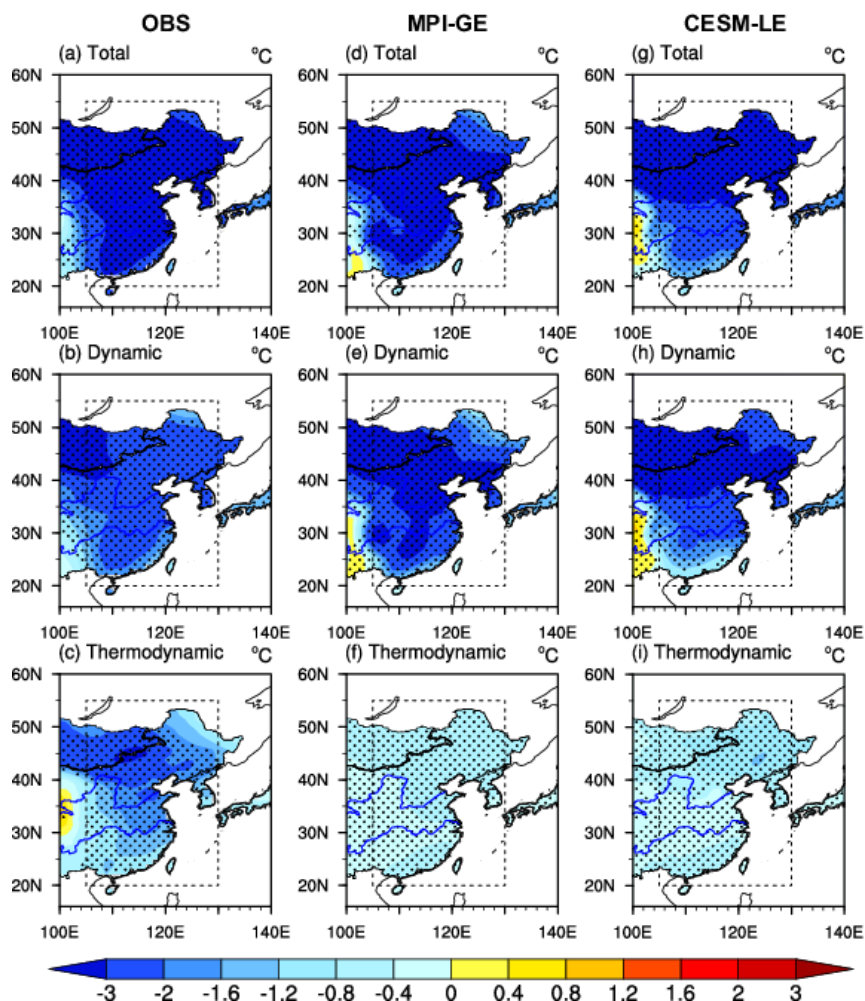


628

629 **Figure 1** Time series decomposition of winter monthly surface air temperature (SAT)  
630 anomalies averaged over East Asia (20°N-55°N and from 105°E-130°E) from the  
631 observation into internal, forced, dynamic and thermodynamic components: (a) total,  
632 (b) dynamic, (c) internally dynamic, (d) forced dynamic and (e) thermodynamic  
633 components. The blue dots represent the cold months in the period of 1962-2011 boreal  
634 winter.

635





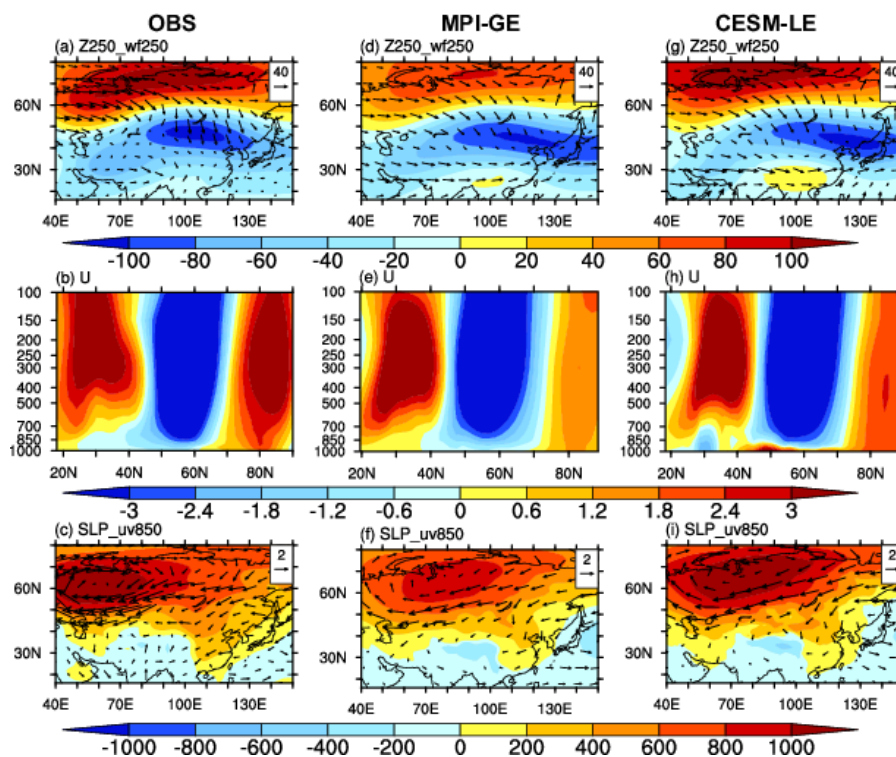
636

637 **Figure 2** The composites of the cold-month SAT anomaly (relative to the 1986-2005  
638 boreal winter climatology) in the observation during the period of 1962-2011 boreal  
639 winter: (a) total, (b) dynamically-induced and (c) thermodynamically-induced. The  
640 subplots (d)-(f) and (g)-(i) correspond to subplots (a)-(c), but for the results in the MPI-  
641 GE and the CESM-LE, respectively. The dotted areas are statistically significant at the  
642 5% level according to Student's t test. The cold months are defined as months in which  
643 SAT is lower than the statistical 5<sup>th</sup> percentile of all the monthly SAT samples during

<https://doi.org/10.5194/egusphere-2023-2806>  
Preprint. Discussion started: 14 December 2023  
© Author(s) 2023. CC BY 4.0 License.

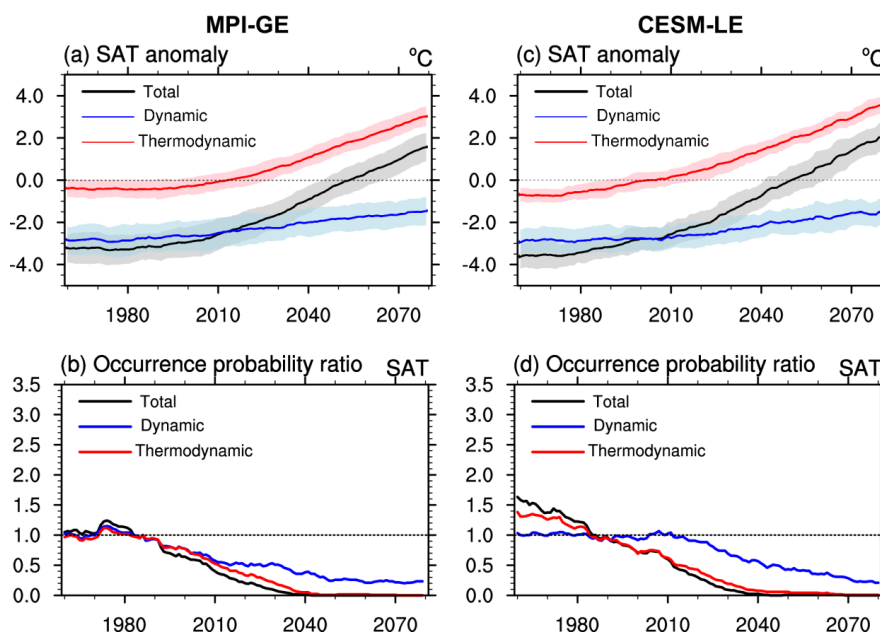


644 1962-2011 boreal winter.



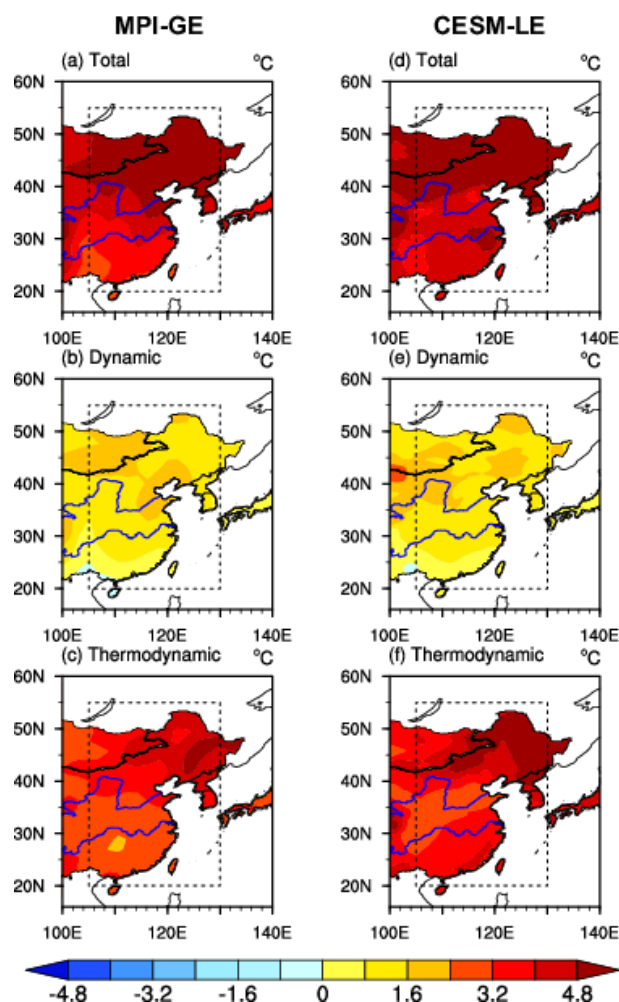
645

646 **Figure 3** Observed composite circulation anomalies (relative to the 1986-2005 boreal  
 647 winter climatology) for East Asian cold extremes during the period of 1962-2011 boreal  
 648 winter: (a) Geopotential height (shading; unit: m) and horizontal components of the  
 649 wave activity flux ( $\text{m}^2 \text{s}^{-2}$ ) at 250-hPa. (b) Zonal mean zonal wind over the vertical cross  
 650 section (zonally averaged over 70-120°E; unit:  $\text{m s}^{-1}$ ); (c) sea level pressure (shading;  
 651 unit: Pa) and horizontal wind at 850-hPa ( $\text{m s}^{-1}$ ). Subplots (d)-(f) and (g)-(i) correspond  
 652 to subplots (a)-(c), but for the results in the MPI-GE and the CESM-LE, respectively.



653

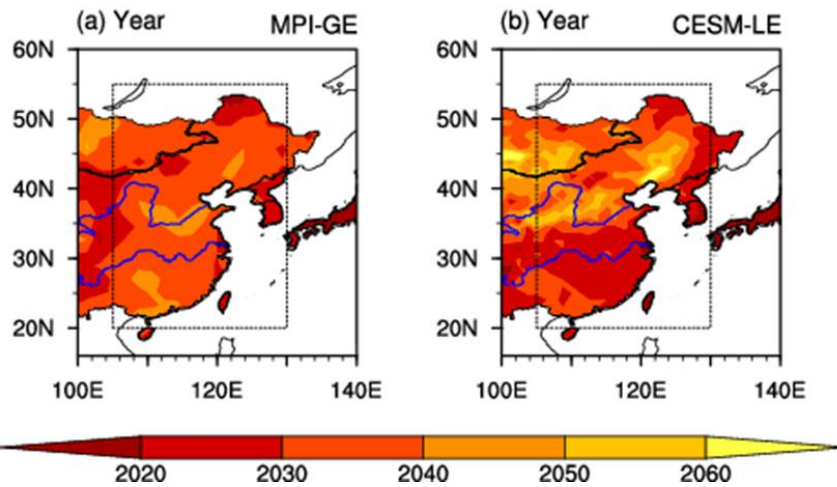
654 **Figure 4** (a) Time series of the 20-yr running averaged cold-month SAT anomaly (black)  
655 and its dynamically-induced (blue) and thermodynamically-induced (red) components  
656 over East Asia relative to the 1986-2005 boreal winter climatology in the MPI-GE. The  
657 shading shows the range of two standard deviations among the model members. (b)  
658 Time series of the occurrence probability ratio of the present-day East Asian cold  
659 extremes in the MPI-GE: both dynamic and thermodynamic components change  
660 (black), only dynamic component changes (blue) and only thermodynamic component  
661 change (red). Subplots (c) and (d) correspond to subplots (a) and (b), but for the results  
662 in the CESM-LE. cold months are defined as the months in which the regional mean  
663 SAT is lower than the statistical 5<sup>th</sup> percentile of the climatological monthly SAT series  
664 during DJF in a certain time slice.



665

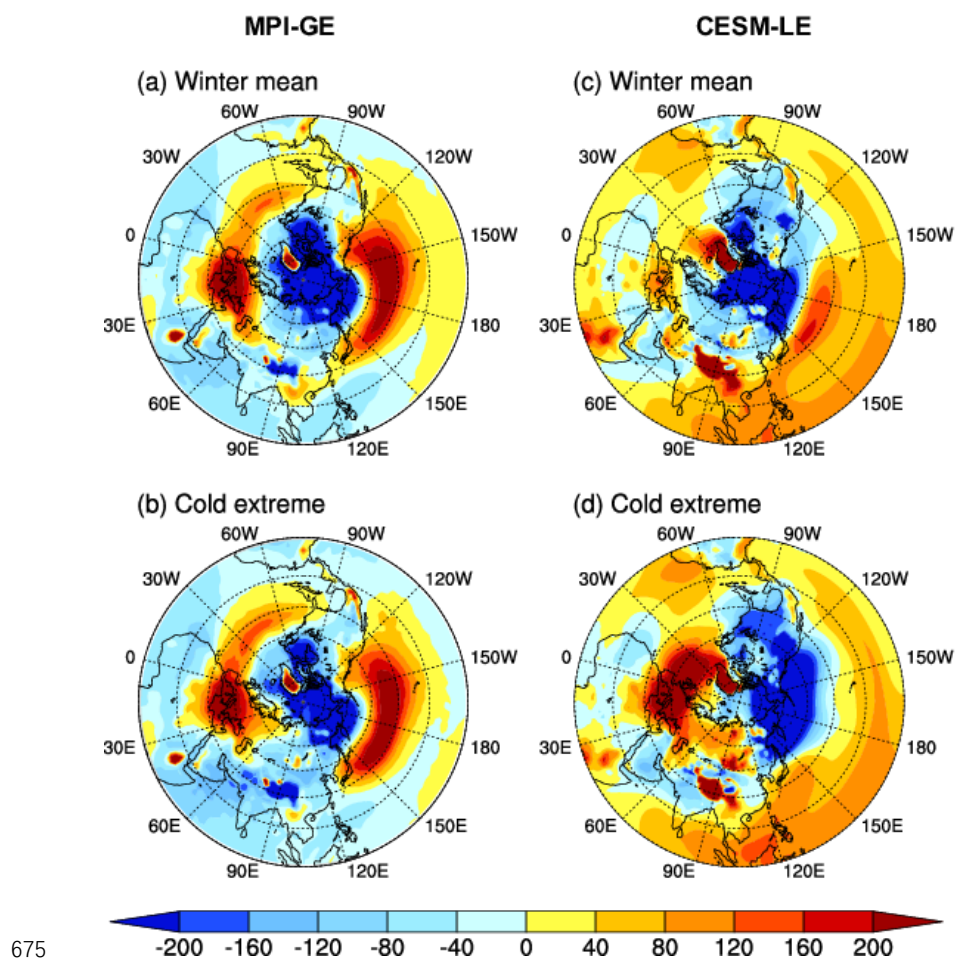
666 **Figure 5** Changes in East Asian cold-month SAT in the MPI-GE in 2079-2098 boreal  
667 winter relative to 1986-2005 boreal winter: (a) Total, (b) dynamic component and (c)  
668 thermodynamic component. Subplots (d)-(f) correspond to subplots (a)-(c), but for the  
669 results in the CESM-LE.

670



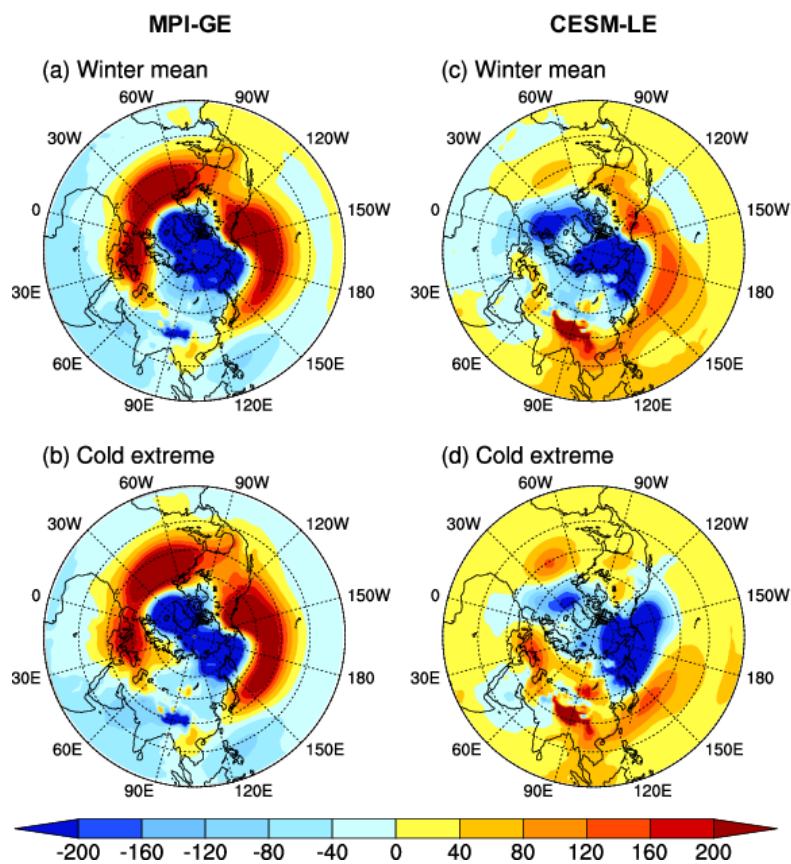
671

672 **Figure 6** The year when the occurrence probability ratio of the present-day (1986-2005  
673 boreal winter) East Asian cold extremes decreases to zero in (a) The MPI-GE and (b)  
674 the CESM-LE.



676 **Figure 7** Changes in SLP for (a) total winter months and (b) cold months in 2079-2098  
677 boreal winter relative to 1986-2005 boreal winter in the MPI-GE. Subplots (c) and (d)  
678 correspond to subplots (a) and (b), but for the results in the CESM-LE.





679

680 **Figure 8** Changes in the dynamic component of SLP for (a) total winter months and (b)  
681 cold months in 2079-2098 boreal winter relative to 1986-2005 boreal winter in the MPI-  
682 GE. Subplots (c) and (d) correspond to subplots (a) and (b), but for the results in the  
683 CESM-LE.

684